

Induction Heating of Cylindrical Billets in Magnetic Field Produced by Permanent Magnets: Simulation and Experiments

Abstract. A complete overview of results is presented concerning induction heating of nonmagnetic cylindrical billets in magnetic field produced by permanent magnets. The authors proposed and modelled two possible ways of the process. The billet either rotates inside a system of appropriately arranged static permanent magnets or a ring containing such magnets rotates around an unmoving billet. Both arrangements were modelled numerically using fully adaptive higher-order finite element method and some results were verified by experiments on a physical model built in our lab.

Streszczenie. W pracy opisano rezultaty modelowania procesu nagrzewania indukcyjnego kęsów aluminiowych w polu magnetycznym wytwarzanym przez magnesy stałe. Autorzy proponują i modelują dwa warianty technologii. Kęs może być obracany wewnętrz zestawu odpowiednio ustawionych magnesów lub pierścień magnesów jest obracany względem nieruchomego kęsa. Oba warianty były symulowane przy pomocy w pełni adaptacyjnej metody elementów skończonych wyższych rzędów. Niektóre wyniki symulacji porównano z modelem fizycznym zbudowanym przez autorów. (*Indukcyjne nagrzewanie cylindrycznych kęsów w polu magnesów trwałych: symulacje i eksperymenty*)

Keywords: induction heating, nonmagnetic billets, higher-order finite element method, magnetic field, temperature field

Słowa kluczowe: nagzewanie indukcyjne, kęsy aluminiowe, MES wyższego rzędu, pole magnetyczne, pole temperatury

Introduction

Induction heating of cylindrical aluminum billets belongs to heat treatment technologies used for their softening before consequent hot forming. As the classical techniques are characterized by rather low efficiencies, novel, much more advantageous processes of this kind are introduced nowadays. One of them is based on heating a billet in magnetic field generated by appropriately arranged permanent magnets. Two possibilities were taken into account: the billet either rotates inside a static ring containing magnetic circuit with built-in permanent magnets or, vice versa, a well dynamically balanced ring containing permanent magnets rotates around the static billet (see Figs. 1a and 1b). While the former arrangement is simpler from the viewpoint of its structure and possibility of driving, the latter one is advantageous from the viewpoint of the manipulation with the billet and lower thermal losses (the surface of the billet is not cooled so intensively because the billet does not move).

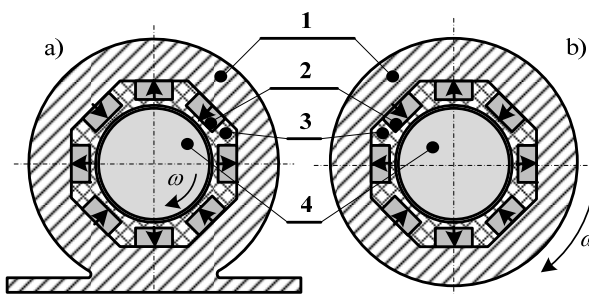


Fig. 1. Arrangement with rotating billet a) and rotating ring with permanent magnets b): 1-magnetic circuit (carbon steel), 2-permanent magnets, 3-thermal insulation, 4-nonmagnetic billet

The paper represents a natural continuation of work [1] and summarizes the most important latest results in the domain achieved by the authors.

Continual mathematical model and its solution

The mathematical model of the process consists of two partial differential equations for the distribution of magnetic and temperature fields in the system. Distribution of magnetic field described by the magnetic vector potential \mathbf{A} obeys the equation [1]

$$(1) \quad \operatorname{curl} \left(\frac{1}{\mu} \operatorname{curl} \mathbf{A} - \mathbf{H}_c \right) - \gamma \mathbf{v} \times \operatorname{curl} \mathbf{A} = \mathbf{0},$$

where μ is the magnetic permeability, γ denotes the electrical conductivity, \mathbf{v} is the local velocity of rotation, and \mathbf{H}_c stands for the coercive force (only in the domain of the permanent magnets). The artificial boundary is characterized by the Dirichlet condition $\mathbf{A} = \mathbf{0}$.

The distribution of temperature in the system is described by the equation [2]

$$(2) \quad \operatorname{div} (\lambda \operatorname{grad} T) = \rho c_p \cdot \left(\frac{\partial T}{\partial t} + \mathbf{v} \cdot \operatorname{grad} T \right) - p,$$

where λ denotes the thermal conductivity, ρ is the specific mass, and c_p stands for the specific heat at a constant pressure. Finally, the symbol p denotes the time average internal sources of heat represented by the volumetric Joule losses (no hysteresis losses are considered). These are given by the formula

$$(3) \quad p = \frac{|\mathbf{J}_{\text{eddy}}|^2}{\gamma}, \quad \mathbf{J}_{\text{eddy}} = \gamma \mathbf{v} \times \operatorname{curl} \mathbf{A}.$$

Equation (2) is supplemented with the boundary condition respecting both convection and radiation.

The physical parameters of heated aluminum (in our case electric and thermal conductivities and heat capacity) are temperature-dependent functions, which must be respected in the model.

Numerical solution

The procedure of the numerical solution starts with rewriting equations (1) and (2) into the weak forms

$$(4) \quad \begin{aligned} & \int_{\Omega} \frac{1}{\mu} \left(\frac{\partial A_z}{\partial x} \cdot \frac{\partial w}{\partial x} + \frac{\partial A_z}{\partial y} \cdot \frac{\partial w}{\partial y} \right) dS + \\ & + \int_{\Omega} \gamma \left(A_z v_x \frac{\partial w}{\partial x} + A_z v_y \frac{\partial w}{\partial y} \right) dS = \\ & = - \int_{\Omega} \frac{1}{\mu} \left(B_{r,y} \frac{\partial w}{\partial x} - B_{r,x} \frac{\partial w}{\partial y} \right) dS - \int_{\Gamma} (Kw) dl \end{aligned}$$

and

$$(5) \quad \int_{\Omega} \lambda \left(\frac{\partial T}{\partial x} \cdot \frac{\partial w}{\partial x} + \frac{\partial T}{\partial y} \cdot \frac{\partial w}{\partial y} \right) dS + \int_{\Omega} \rho c_p \frac{\partial T}{\partial t} w dS - \\ - \int_{\Omega} \rho c_p T \left(v_x \frac{\partial w}{\partial x} + v_y \frac{\partial w}{\partial y} \right) dS + \\ + \int_{\Gamma} \alpha T w dl = \int_{\Omega} p_j w dS + \int_{\Gamma} (\alpha T_0 + g) w dl$$

The solution itself is realized by a fully adaptive higher-order finite element method, whose algorithms are implemented into codes Agros2D [3] and Hermes2D [4]. Both codes developed in our group for about ten years and written in C++ are generally intended for monolithic numerical solution of systems of generally nonlinear and nonstationary second-order partial differential equations and they are mainly used for hard-coupled modeling of complex physical problems. While Hermes2D is a library containing the most advanced procedures and algorithms for the numerical processing of the task solved, Agros2D represents a powerful preprocessor and postprocessor. Both codes are freely distributable and in 2D version they exhibit a lot of unique features, such as fully automatic *hp*-adaptivity, work with hanging nodes of any level, multimesh technology (every field can be calculated on a different mesh generally varying in time) and a possibility of combining triangular, quadrilateral and curved elements.

Illustrative example obtained results

The mathematical model was tested on a device built in our laboratory. The device (corresponding to the version in Fig. 1 left) is depicted in Fig. 2. The principal dimensions of the heating part are indicated in Fig. 3.

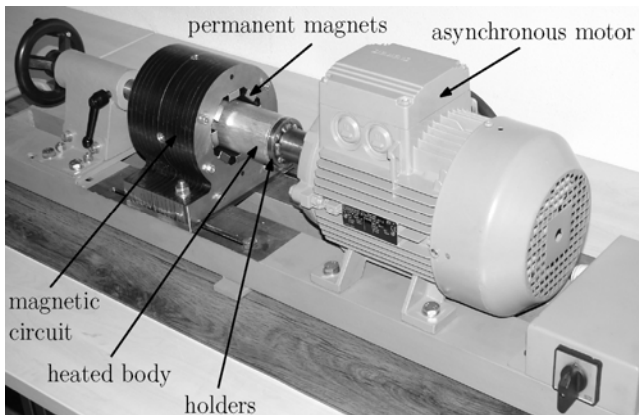


Fig. 2. Device for induction heating of rotating aluminum billets up to $\varnothing 60$ mm

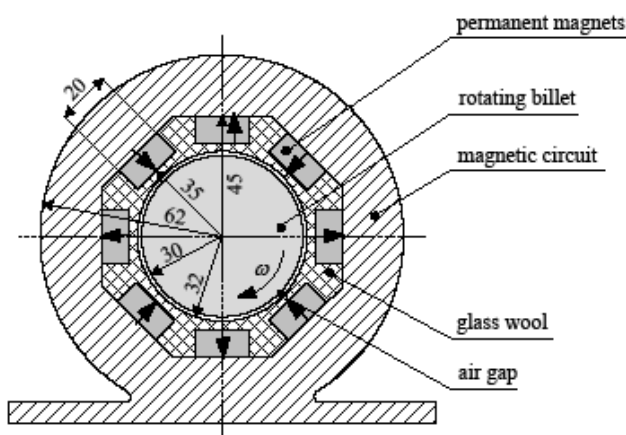


Fig. 3. Principal dimensions (in mm) of the heating part

The rated revolutions of the billet are $n = 1500$ rpm, the corresponding angular velocity $\omega = 157.1$ rad/s. The magnetic circuit is made of carbon steel CSN 12 040 (its magnetization characteristic is in Fig. 4), permanent magnets are of type VMM10 (cross section of one magnet is 20×10 mm, $B_r = 1.28$ T, and $\mu_r = 1.11$). The permanent magnets must be protected from excessive temperatures in order to avoid deteriorating their magnetic properties ($T_{max} = 80$ °C). This protection is realized by glass wool, which is a good thermal insulation. The axial length of the system is 120 mm.

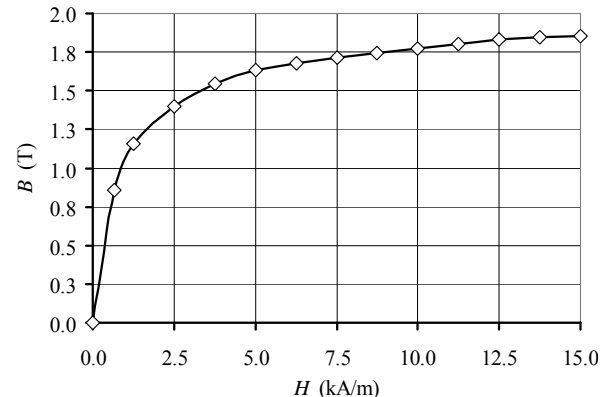


Fig. 4. Magnetization characteristic of steel 12 040

Figure 5 shows the discretization mesh (at the end of the process of adaptivity) used for computation of magnetic field in the system. The numbers in the rectangles denote the degrees of polynomials in particular elements.

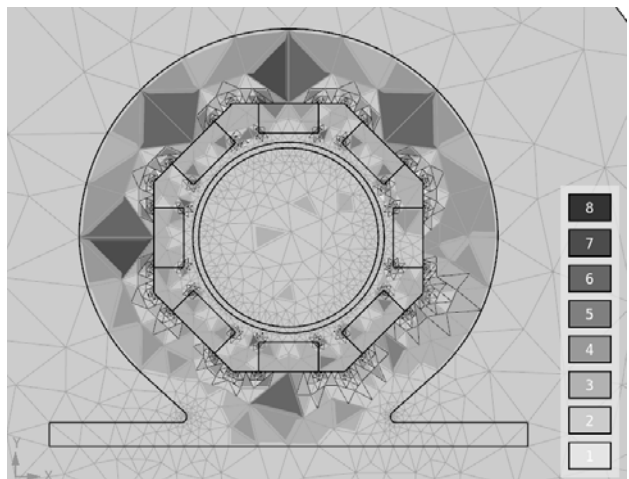


Fig. 5. Discretization mesh: the billet is discretized using curved elements (light lines - before adaptivity, dark lines - after adaptivity, numbers in the right column show the orders of the elements)

The billet is discretized by combination of triangular and curvilinear elements. The regions in the neighborhood of the corners of the magnetic circuit representing the singular points are discretized by small triangles of low polynomial orders while places with expected smooth regions are covered by large triangles of high polynomial orders.

Figure 6 shows the convergence curves when using the triangular and curvilinear elements for different initial setting of approximating polynomials in particular cells of the mesh. Comparable results are obtained (after the process of adaptivity) for 1396 elements (some of them being curved) and 1824 purely triangular elements. The savings in DOFs in this case are about 30 %.

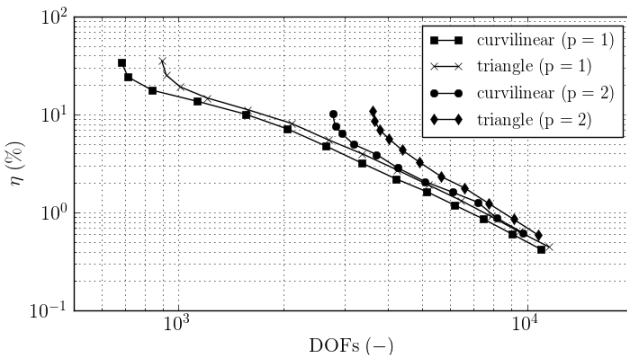


Fig. 6. Convergence curves of results: symbol p denotes the initial degree of polynomials before the adaptive process (Agros2D)

The distribution of force lines in the cross section of the system for the initial temperature and nominal revolutions is depicted in Fig. 6.

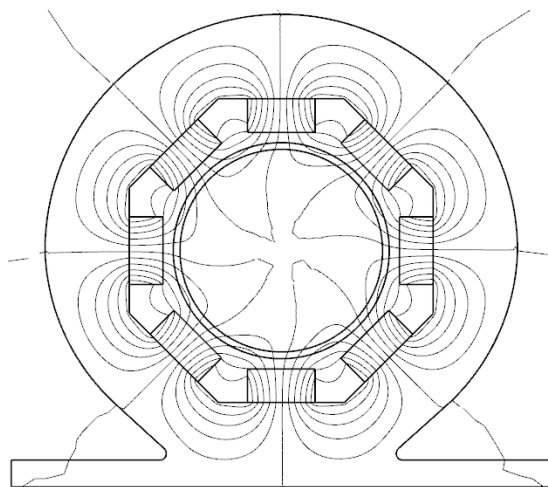


Fig. 7: Distribution of magnetic field in the system

The distribution of temperature in the system after 120 s of heating is depicted in Fig. 8. While the temperature of the billet reaches about 170 °C (and is almost uniform), due to the presence of good thermal insulation the permanent magnets (and also magnetic circuit) remain cold, so that there is no danger of deteriorating their physical properties because of overheating. The initial temperature of the heating process $T_0 = 30$ °C.

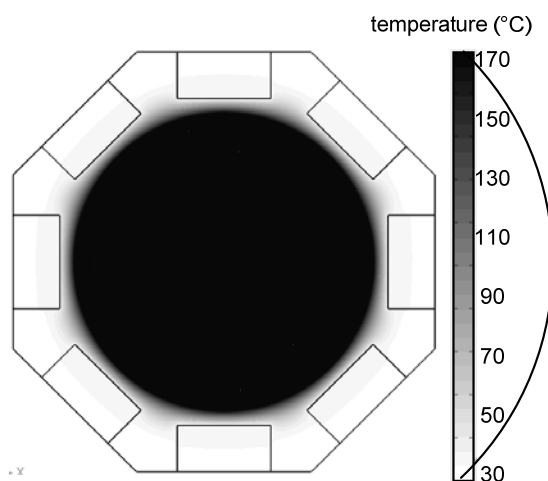


Fig. 8. Distribution of the temperature in the system after 120 s of heating ($n = 1500$ rpm)

Figure 9 contains the comparison between the calculated and measured temperatures of the billet surface versus time. There are two characteristics. The upper one corresponds to eight permanent magnets, while the lower one was obtained for only four magnets (instead of four remaining magnets the model contained four ferromagnetic poles of the same dimensions). The agreement is very good.

The measurement of the surface temperature was performed using a high-quality thermocamera Fluke. The results of several measurements were averaged.

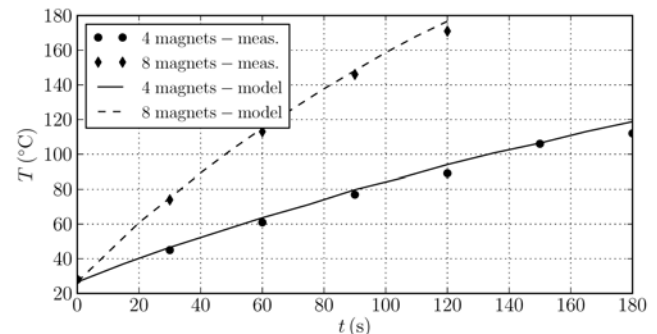


Fig. 9. Time evolution of the average temperature of the billet for $n = 1500$ rpm

Analogous computations were carried out for the version depicted in Fig. 1 left (with a rotating ring with permanent magnets). Due to lower coefficient of the convective heat transfer the results are more favourable, see Fig. 10.

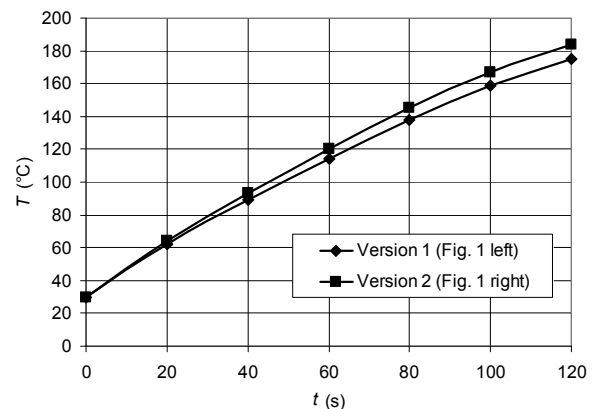


Fig. 10. Time evolution of the average temperature of the billet for both versions depicted in Fig. 1

Acknowledgment

The financial support of the Grant Agency of the Czech Republic (projects No. 102/10/0216 and 102/11/0498) is highly acknowledged.

REFERENCES

- [1] Karban, P., Mach, F., Doležel, I.: Hard-Coupled Model of Induction Heating of Cylindrical Nonmagnetic Billets Rotating in System of Permanent Magnets. Electrical Review 87, No. 12b, 2011, pp. 78–81.
- [2] Holman, J. P.: Heat Transfer, McGrawHill, New York, NY, USA, 2001.
- [3] <http://agros2d.org>.
- [4] <http://hpfem.org/hermes>.

Authors: Prof. Ivo Doležel, Ing. František Mach, Assoc. Prof. Pavel Karban, University of West Bohemia in Pilsen, Faculty of Electrical Engineering, Univerzitní 26, 30614 Plzeň, Czech Republic, E-mail: {idolezel, fmach, karban}@kte.zcu.cz; Ing. Lubomír Musálek, Czech Technical University, Faculty of Electrical Engineering, Technická 2, 166 27 Praha, Czech Republic, E-mail: {musallub}@fel.cvut.cz.